

## University of Groningen

### The antifibrotic potential of a sustained release formulation of a PDGF beta-receptor targeted rho kinase inhibitor

van Dijk, F.; Teekamp, N.; Post, E.; Schuppan, D.; Kim, Y. O.; Zuidema, J.; Steendam, R.; Klose, Matthias H. M. ; Meier-Menches, Samuel M. ; Casini, A.

*Published in:*  
Journal of Controlled Release

*DOI:*  
[10.1016/j.jconrel.2018.12.039](https://doi.org/10.1016/j.jconrel.2018.12.039)

**IMPORTANT NOTE:** You are advised to consult the publisher's version (publisher's PDF) if you wish to cite from it. Please check the document version below.

*Document Version*  
Publisher's PDF, also known as Version of record

*Publication date:*  
2019

[Link to publication in University of Groningen/UMCG research database](#)

*Citation for published version (APA):*

van Dijk, F., Teekamp, N., Post, E., Schuppan, D., Kim, Y. O., Zuidema, J., Steendam, R., Klose, M. H. M., Meier-Menches, S. M., Casini, A., Horvatovich, P. L., Sijbrandi, N. J., Frijlink, H. W., Hinrichs, W. L. J., Poelstra, K., Beljaars, L., & Olinga, P. (2019). The antifibrotic potential of a sustained release formulation of a PDGF beta-receptor targeted rho kinase inhibitor. *Journal of Controlled Release*, 296, 250-257. <https://doi.org/10.1016/j.jconrel.2018.12.039>

#### Copyright

Other than for strictly personal use, it is not permitted to download or to forward/distribute the text or part of it without the consent of the author(s) and/or copyright holder(s), unless the work is under an open content license (like Creative Commons).

The publication may also be distributed here under the terms of Article 25fa of the Dutch Copyright Act, indicated by the "Taverne" license. More information can be found on the University of Groningen website: <https://www.rug.nl/library/open-access/self-archiving-pure/taverne-amendment>.

#### Take-down policy

If you believe that this document breaches copyright please contact us providing details, and we will remove access to the work immediately and investigate your claim.

Downloaded from the University of Groningen/UMCG research database (Pure): <http://www.rug.nl/research/portal>. For technical reasons the number of authors shown on this cover page is limited to 10 maximum.



# The antifibrotic potential of a sustained release formulation of a PDGF $\beta$ -receptor targeted rho kinase inhibitor

F. van Dijk<sup>a,b</sup>, N. Teekamp<sup>a</sup>, E. Post<sup>b</sup>, D. Schuppan<sup>c,d</sup>, Y.O. Kim<sup>c</sup>, J. Zuidema<sup>e</sup>, R. Steendam<sup>e</sup>, Matthias H.M. Klose<sup>i</sup>, Samuel M. Meier-Menchies<sup>f,i</sup>, A. Casini<sup>f</sup>, P.L. Horvatovich<sup>g</sup>, N.J. Sijbrandi<sup>h</sup>, H.W. Frijlink<sup>a</sup>, W.L.J. Hinrichs<sup>a</sup>, K. Poelstra<sup>b</sup>, L. Beljaars<sup>b</sup>, P. Olinga<sup>a,\*</sup>

<sup>a</sup> Groningen Research Institute of Pharmacy, Department of Pharmaceutical Technology and Biopharmacy, University of Groningen, Groningen, The Netherlands

<sup>b</sup> Groningen Research Institute of Pharmacy, Department of Pharmacokinetics, Toxicology and Targeting, University of Groningen, Groningen, The Netherlands

<sup>c</sup> Institute of Translational Immunology and Research Center for Immune Therapy, University Medical Center, Johannes Gutenberg University, Mainz, Germany

<sup>d</sup> Beth Israel Deaconess Medical Center, Harvard Medical School, Boston, MA, USA

<sup>e</sup> InnoCore Pharmaceuticals, Groningen, The Netherlands

<sup>f</sup> School of Chemistry, Cardiff University, Park Place, CF10 3AT, Cardiff, UK

<sup>g</sup> Groningen Research Institute of Pharmacy, Department of Analytical Biochemistry, University of Groningen, Groningen, the Netherlands

<sup>h</sup> LinXis BV, Amsterdam, The Netherlands

<sup>i</sup> Department of Analytical Chemistry, University of Vienna, Waehringer StraÙe 38, 1090 Vienna, Austria

## ARTICLE INFO

### Keywords:

Controlled release  
Polymeric microspheres  
Protein delivery  
Drug targeting  
Biologicals  
Liver fibrosis

## ABSTRACT

Rho kinase activity in hepatic stellate cells (HSCs) is associated with activation, transformation and contraction of these cells, leading to extracellular matrix production and portal hypertension in liver cirrhosis. Inhibition of rho kinase activity can reduce these activities, but may also lead to side effects, for instance systemic hypotension. This can be circumvented by liver-specific delivery of a rho kinase inhibitor to effector cells. Therefore, we targeted the rho kinase inhibitor Y27632 to the key pathogenic cells in liver fibrosis, i.e. myofibroblasts including activated HSCs that highly express the PDGF $\beta$ -receptor, using the drug carrier pPB-MSA. This carrier consists of mouse serum albumin (MSA) covalently coupled to several PDGF $\beta$ R-recognizing moieties (pPB). We aimed to create a prolonged release system of such a targeted construct, by encapsulating pPB-MSA-Y27632 in biodegradable polymeric microspheres, thereby reducing short-lasting peak concentrations and the need for frequent administrations. Firstly, we confirmed the vasodilating potency of PDGF $\beta$ -receptor targeted Y27632 *in vitro* in a contraction assay using HSCs seeded on a collagen gel. We subsequently demonstrated the *in vivo* antifibrotic efficacy of pPB-MSA-Y27632-loaded microspheres in the Mdr2<sup>-/-</sup> mouse model of progressive biliary liver fibrosis. A single subcutaneous microsphere administration followed by organ harvest one week later clearly attenuated liver fibrosis progression and significantly suppressed the expression of fibrosis related genes, such as several collagens, profibrotic cytokines and matrix metalloproteinases. In conclusion, we demonstrate that polymeric microspheres are suitable as drug delivery system for the sustained systemic delivery of targeted protein constructs with antifibrotic potential, such as pPB-MSA-Y27632. This formulation appears suitable for the sustained treatment of liver fibrosis and possibly other chronic diseases.

## 1. Introduction

In advanced liver fibrosis, scarring and contraction of fibrogenic cells leads to portal hypertension due to increased hepatic resistance to portal inflow, representing one of the major complications of cirrhosis [1,2]. On the other hand, cirrhosis is commonly associated with a reduced mean arterial pressure due to peripheral vasodilation, causing an increase in splanchnic flow, which severely compromises options for

treatment [2,3].

Upregulation of intrahepatic rho-associated protein kinase activity (here termed rho kinase), contributes to the development of portal hypertension in liver cirrhosis [4,5]. Rho kinase is a major downstream effector protein of Rho GTPase, and is involved in cell migration and contractility of different cell types [6,7]. Inhibition of this protein using rho kinase inhibitors, such as Y27632, reduced portal vascular resistance and thus portal pressure [5,8]. In addition to these

\* Corresponding author.

E-mail address: [p.olinga@rug.nl](mailto:p.olinga@rug.nl) (P. Olinga).

<https://doi.org/10.1016/j.jconrel.2018.12.039>

Received 8 June 2018; Received in revised form 29 November 2018; Accepted 21 December 2018

Available online 22 January 2019

0168-3659/ © 2019 The Author(s). Published by Elsevier B.V. This is an open access article under the CC BY-NC-ND license (<http://creativecommons.org/licenses/by-nc-nd/4.0/>).

hemodynamic effects, Y27632 was shown to possess antifibrotic activity in several animal models of liver fibrosis [9–11]. However, systemic administration of a rho kinase inhibitor will affect many cell types in different organs, as rho kinase-controlled signaling occurs in virtually every cell type. This may cause adverse effects, including a reduction in vascular smooth muscle contractility and therefore a further decline in the already low systemic blood pressure in cirrhotics [8,12].

This side effect can be circumvented by the cell-specific delivery of a rho kinase inhibitor to the key pathogenic organ and cells, preventing effects on other cells such as vascular smooth muscle cells. The pathogenic cells involved in the excessive production of extracellular matrix (ECM) proteins in liver fibrosis are hepatic stellate cells (HSCs) and myofibroblasts that show a contractile phenotype [13]. These cells can be reached by targeting their exclusively expressed PDGF $\beta$ -receptors with an albumin-based drug carrier (pPB-MSA). pPB-MSA is composed of several PDGF $\beta$ -receptor recognizing peptides (pPB) attached to an albumin core (mouse serum albumin, MSA) [14,15]. By inhibiting rho kinase activity specifically in the target cells, their migration, contraction and excess extracellular matrix production can be impeded. The antifibrotic effect of the rho kinase inhibitor Y27632 when targeted to the myofibroblasts using the similar albumin carrier M6P-HSA binding to the mannose 6-phosphate/insulin-like growth factor II (M6P/IGFII) receptor was previously demonstrated [7]. The inhibitor was coupled to the carrier via a platinum-based linker, allowing slow intracellular release of Y27632 from the conjugate during several days after endocytic uptake [7,16]. The same rho kinase inhibitor and linker were successfully used before to target the fibrotic kidney [17].

An essential challenge in the application of therapeutic proteins is the route of administration. For such drugs the most common route is parenteral administration, generally causing undesirable fluctuations in plasma levels and moreover the need for repeated parenteral injections; a high burden to the patient [18]. Therefore, in addition to the formation of an intracellular slow release depot of Y27632 by taking advantage of the properties of the chemical linker, a patient-friendly formulation providing gradual and prolonged release of such therapeutic proteins for application in chronic diseases such as fibrosis may ensure sustained release [19]. We previously established the sustained controlled release of a similar albumin-based carrier lasting for at least 7 days *in vivo* by encapsulating the protein in biodegradable polymeric microspheres [20] and explored the pharmacokinetic release profile [15]. We were able to demonstrate long lasting serum levels of the carrier and its localization in the fibrotic organ.

In the present study, we explored the pharmacodynamic properties of biodegradable polymeric microspheres loaded with the albumin-based carrier (pPB-MSA) coupled to an antifibrotic compound (Y27632) via the platinum-based Lx-linker. We first assessed the relaxing potential of pPB-MSA-Y27632 *in vitro*. Subsequently, we prepared polymeric microspheres containing pPB-MSA-Y27632 that allow release of proteins for at least 7 days and confirmed its antifibrotic activity at 7 days after a single microsphere injection in Mdr2 $^{-/-}$  mice with progressive biliary liver fibrosis.

## 2. Materials and methods

### 2.1. Synthesis and characterization of proteins

pPB-MSA was synthesized as described in the supplemental materials and methods [14,15]. The Lx-linker (LinXis, Amsterdam, the Netherlands) was used as platinum-based linker to couple Y27632 to pPB-MSA. The Lx-linker was conjugated to *trans*-4-[(1*R*)-1-Aminoethyl]-*N*-4-pyridinylcyclohexanecarboxamide dihydrochloride, *i.e.* Y27632 (Tocris Bioscience, Bristol, UK), and characterized with NMR, mass spectrometry and HPLC as described in the supplemental materials and methods, and was subsequently coupled to pPB-MSA. In short,

0.214  $\mu$ mol Y27632-Lx reacted with 14 nmol pPB-MSA in 20 mM tricine/NaNO<sub>3</sub> buffer pH 8.5 for 30 min at room temperature while stirring, and subsequently incubated overnight at 37 °C. The mixture was dialyzed against PBS for 48 h, and freeze dried.

The product was characterized by silver staining and MALDI-TOF mass spectrometry (Voyager DE-Pro MALDI-TOF, Applied Biosystems, Foster City, CA, USA) in a sinapinic acid matrix according to standard protocols. The molecular weight range was estimated from the obtained spectra at a cutoff of 30% of the maximum intensity, at which the background noise was exceeded. For the silver staining, samples (10  $\mu$ g) were applied on a 10% SDS polyacrylamide gel according to standard procedures. In short, the gel was fixed in H<sub>2</sub>O/MeOH = 1/1 containing acetic acid. After washing in 25% EtOH in H<sub>2</sub>O, the gel was incubated in H<sub>2</sub>O containing Na<sub>2</sub>S<sub>2</sub>O<sub>3</sub>. Next, the gel was extensively washed in H<sub>2</sub>O, incubated in H<sub>2</sub>O supplemented with AgNO<sub>3</sub> and formaldehyde, washed again and developed in H<sub>2</sub>O containing Na<sub>2</sub>S<sub>2</sub>O<sub>3</sub>, formaldehyde and Na<sub>2</sub>CO<sub>3</sub>. The reaction was stopped by washing and subsequent incubation in H<sub>2</sub>O/MeOH = 4/5 containing acetic acid, after which the gel was photographed.

### 2.2. Contraction assay

Human LX2 hepatic stellate cells were kindly provided by Prof. Scott Friedman (Mount Sinai Hospital, New York) and cultured in Dulbecco's modified Eagle's medium (DMEM, Invitrogen, Carlsbad, CA) supplemented with 10% FCS and antibiotics (100 U/ml penicillin and 100  $\mu$ g/ml streptomycin). Cells (50,000/well) were seeded in complete medium containing 2% FCS on collagen gels, composed of 1.2 mg/ml collagen I (rat tail, Corning, New York), 6 mM NaOH, 0.4  $\times$  PBS (55 mM NaCl, 1 mM KCl, 4 mM PO<sub>4</sub><sup>3-</sup>, pH 7.4) and 20 mM HEPES diluted in medium, which were allowed to solidify for 1 h at 37 °C and 5% CO<sub>2</sub>. After 3 h, the medium was replaced by complete medium and cells incubated with 10  $\mu$ M Y27632, pPB-MSA-Y27632 or pPB-MSA for 48 h. Gels were photographed and contraction was determined as the ratio between the surface of the gel and the surface of the well as measured with ImageJ (National Institutes of Health, USA).

### 2.3. Production and characterization of microspheres

Microspheres were produced using a similar double emulsification evaporation method as described previously [20]. The used polymers are phase-separated multi-block copolymers, composed of poly(L-lactide) (PLLA), poly ethylene glycol (PEG) and poly( $\epsilon$ -caprolactone) (PCL). The copolymers [PCL-PEG<sub>1000</sub>-PCL]-[PLLA] (50/50 weight ratio) and [PCL-PEG<sub>3000</sub>-PEG]-[PLLA] (30/70 weight ratio) (obtained from InnoCore Pharmaceuticals, Groningen, The Netherlands) were used at a 1:1 weight ratio. PBS (control), or pPB-MSA-Y27632 and MSA in a 1:4 weight ratio, or pPB-MSA and MSA in a 3:2 weight ratio were encapsulated at a 5 wt-% theoretical protein load. Microspheres were characterized for morphology by scanning electron microscopy, particle size distribution by laser diffraction, protein content and *in vitro* protein release as described before by Teekamp et al. [20].

### 2.4. Animal experiments

Experiments with the Mdr2 $^{-/-}$  mouse model were approved by the Animal Ethical Committee of the State of Rhineland Palatinate. Female FVB mice ( $n$  = 8) were purchased from Jackson Laboratory (Jackson Laboratory, Bar Harbor, ME, USA) and FVB Mdr2 $^{-/-}$  mice ( $n$  = 26) (20–26 g) were bred in homozygosity at the Institute of Translational Immunology at Mainz University Medical Center. All animals were housed with a 12 h light/dark cycle with *ad libitum* chow and water. At age 8–9 weeks, Mdr2 $^{-/-}$  mice were injected subcutaneously in the neck. Mice received 500  $\mu$ l of 0.4% carboxymethyl cellulose (CMC, Aqualon high M<sub>w</sub>, Ashland, pH 7.0–7.4) containing either 63 mg microspheres encapsulating 3 wt-% pPB-MSA + 2 wt-%

MSA ( $n = 8$ ), or 100 mg microspheres encapsulating 1 wt-% pPB-MSA-Y27632 + 4 wt-% MSA ( $n = 4$ ) or no protein (polymer only) ( $n = 8$ ). Another group of mice was injected subcutaneously once daily for 7 days with 250  $\mu\text{g}/\text{ml}$  Y27632 (Tocris Bioscience, Bristol, UK) in PBS for a final dose of 1 mg/kg ( $n = 6$ ). All mice were sacrificed 7 days after microsphere administration or after 7 injections with plain Y27632. Livers were collected for further analysis.

### 2.5. Inductively coupled plasma mass spectrometry

The platinum content in the livers was quantitated with inductively coupled plasma mass spectrometry (ICP-MS), using an ICP-MS Agilent 7500ce (Agilent Technologies, Waldbronn, Germany) instrument, equipped with a CETAC ASC-520 autosampler (CETAC Technologies, Omaha, Nebraska, USA) and a MicroMist nebulizer at a sample uptake rate of 0.25 ml/min. The instrument was calibrated on a daily basis. Platinum and rhenium standards for ICP-MS measurements were derived from CPI International (Amsterdam, The Netherlands). ICP-MS parameters were: RF power 1560 W, cone material nickel, carrier gas 0.9–1.0 l/min, make up gas 0.2–0.3 l/min, plasma gas 15 l/min, dwell time 0.3 s, replicates 10, monitored isotopes  $^{194}\text{Pt}$  and  $^{195}\text{Pt}$ . The Agilent MassHunter software package (Workstation Software, version B.01.01, Build 123.11, Patch 4, 2012) was used for data processing. Samples were prepared by digestion of 15–30 mg tissue, gravimetrically weighted, in 2 ml 20% nitric acid using a microwave system (Discover SP-D, CEM Microwave Technology, Germany) (200 °C, ramp time 5 min, hold time 6 min, maximal power 300 W). Digested samples were diluted with ultrapure water (18.2 M $\Omega$  cm, Milli-Q Advantage, Darmstadt, Germany) resulting in nitric acid concentrations < 4% and platinum concentrations < 15  $\mu\text{g}/\text{kg}$ .

### 2.6. Low density array

Total RNA was isolated from livers using a Maxwell® LEV simply RNA Cells/Tissue kit (Promega, Madison, WI, USA) according to manufacturer's instructions. RNA concentrations were determined using NanoDrop One spectrophotometer (Thermo Fisher Scientific, Waltham, MA, USA). The expression of 27 fibrosis-related genes (supplementary table 1) was studied with a custom-designed low density array. For this, a reaction mixture containing 50  $\mu\text{l}$  of 6 ng/ $\mu\text{l}$  cDNA and 50  $\mu\text{l}$  2 $\times$  TaqMan PCR Master Mix was loaded per sample. PCR amplification was performed on a ViiA7 Real-Time PCR system (all Applied Biosystems). For each sample, mRNA expression was normalized for GAPDH,  $\beta$ -actin and YWHAZ. Fold induction values were calculated using the  $2^{-\Delta\Delta\text{Ct}}$  method and subsequently Z-normalized [21]. For this, the mean  $2^{-\Delta\Delta\text{Ct}}$  and the standard deviation of the  $2^{-\Delta\Delta\text{Ct}}$  values of each population were calculated. Z-normalization was performed by subtracting the mean from each  $2^{-\Delta\Delta\text{Ct}}$  value in a population, and subsequently dividing these values by the standard deviation. Heat maps for different sets of genes were generated using R Studio (version 1.1.383).

### 2.7. Immunohistochemistry

Paraffin sections of livers were cut with a Leica Reichert-Jung 2040 microtome (Leica Microsystems, Nussloch, Germany) with a thickness of 4  $\mu\text{m}$ . The sections were deparaffinized in xylene and ethanol. Sections were rehydrated in PBS and were incubated for 1 h with the primary antibodies (goat anti-collagen I&III (both 1:200 + 5% normal mouse serum (Southern Biotech, Birmingham, AL, USA)) at room temperature. Next, sections were incubated with the appropriate HRP-conjugated secondary antibody (1:100, DAKO, Santa Clara, CA, USA) for 30 min at room temperature and were visualized with ImmPACT NovaRED (both Vector, Burlingame, CA, USA). Hematoxylin counterstaining was performed. Digital photomicrographs were captured at 400 $\times$  magnification, and quantified using Aperio ImageScope software 12.3.2.8013 (all Aperio, Vista, CA, USA). The total intensity of strong

positive pixels was determined per surface area of liver tissue ( $\mu\text{m}^2$ ), excluding sclerosing bile ducts.

### 2.8. Statistical analyses

At least 3 individual experiments were performed for the *in vitro* microsphere characterization. All data are represented as mean  $\pm$  SEM. The graphs were made with Graphpad Prism version 8 (GraphPad Prism Software, Inc., La Jolla, CA, USA). The statistics were performed with R (version 3.4.0, 2017-04-21, 64 bit). Statistical differences were assessed by Kruskal Wallis test, and if applicable pairwise comparison was done by Mann-Whitney test corrected with Benjamini-Hochberg test, unless stated otherwise in the figure caption.

## 3. Results

### 3.1. Characterization of pPB-MSA-Y27632

The rho kinase inhibitor Y27632 was coupled to pPB-MSA as HSC-selective drug carrier using the platinum-based Lx-linker. Characterization of the constructs using silver staining and MALDI-TOF mass spectrometry showed monomeric protein products with average molecular weights of 66,0 kDa, 71,0 kDa and 73,6 kDa for MSA, pPB-MSA and pPB-MSA-Y27632, respectively (Fig. 1, Table 1, Fig. S1). Based on these data, we calculated that per mouse albumin molecule approximately 5 pPB-moieties (MW = 1 kDa) and 5 Y27632 molecules (MW = 538 Da) were coupled (Table 1).

### 3.2. *In vitro* effect of pPB-MSA-Y27632

To verify the *in vitro* activity of pPB-MSA-Y27632, we assessed the relaxing potency of targeted Y27632 in a contraction assay using LX2 hepatic stellate cells seeded on a collagen gel (Fig. 2A and B), as rho kinase is known to be particularly involved in cell contractility. Both pPB-MSA-Y27632 and free Y27632 (in equimolar amounts) significantly reduced the contractility of LX2 cells after 48 h by  $38.7 \pm 8.4\%$  and  $41.0 \pm 5.5\%$ , respectively. The carrier pPB-MSA alone did not affect cell contraction. These results indicate that PDGF $\beta$ -receptor directed Y27632 is able to exert its effect in the designated target cells.

### 3.3. Microsphere characterization

We continued our studies with the development of a sustained release formulation aiming for at least 7 days of gradual release of pPB-MSA-Y27632. For this, we prepared polymeric microspheres and encapsulated our construct as described before [15,20]. The microspheres displayed a polydisperse size distribution and a median particle size of 27.9  $\mu\text{m}$  (Fig. 3B, Table 2). Control microspheres containing either pPB-MSA or no protein were slightly smaller in size, with median sizes of 21.6 and 22.0  $\mu\text{m}$ , respectively. Scanning electron microscopy showed that all particles were spherical with a smooth surface (Fig. 3A) and

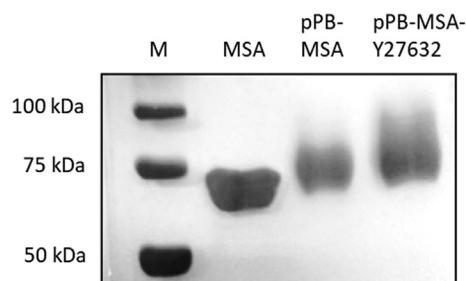
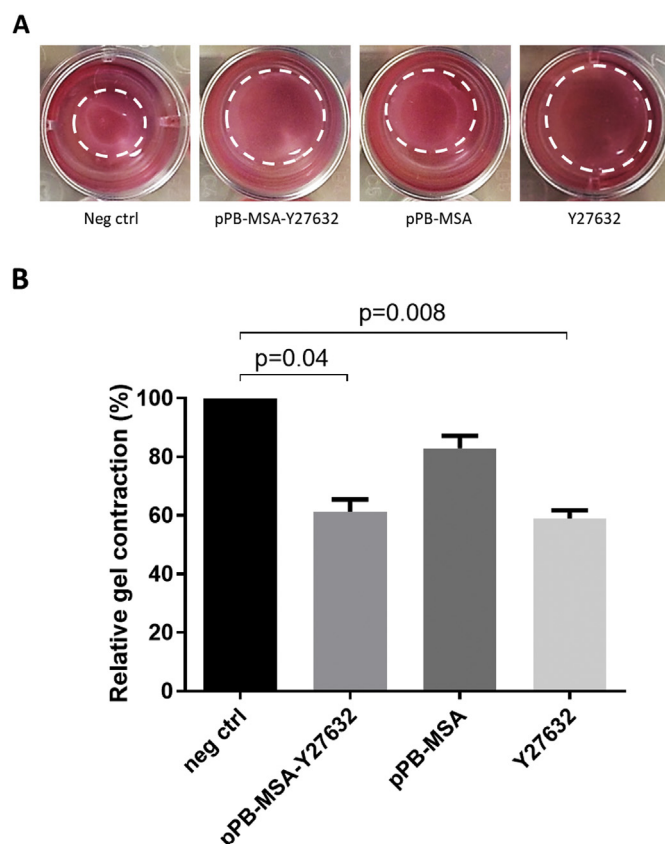


Fig. 1. Analysis of MSA-based protein constructs using silver staining. M denotes molecular weight marker.



**Table 1**  
Characterization of MSA-based protein constructs using MALDI-TOF mass spectrometry. MW denotes molecular weight of the protein constructs.

	Average MW (Da)	Range MW (Da)	# pPB coupled	# Y27632 coupled
MSA	65,950	65,000–66,850	–	–
pPB-MSA	70,950	66,900–77,600	5	–
pPB-MSA-Y27632	73,570	66,150–80,150	5	5



**Fig. 2.** The *in vitro* effect of pPB-MSA-Y27632 as determined by a contraction assay in cultures of LX2 cells seeded on collagen gels. (A) Representative images and (B) analysis of the three-dimensional gel contraction assay following treatment of cells for 48 h with pPB-MSA-Y27632, pPB-MSA or Y27632 ( $n = 4$ ), relative to vehicle treatment. Dashed circles indicate the margins of the gels comprising the gel surface areas. Differences between groups were assessed in Graphpad Prism version 8 by Friedman test followed by Dunn's multiple comparisons test.

analysis of the protein content of the microspheres revealed a high encapsulation efficiency of 81% for pPB-MSA-Y27632-loaded microspheres and 103% for pPB-MSA encapsulated particles (Table 2). The *in vitro* release profile of proteins from the pPB-MSA-Y27632 microspheres revealed sustained and gradual release for several days, with only a minimal initial burst release. The cumulative protein release from pPB-MSA-Y27632-loaded microspheres in release buffer was  $78 \pm 2.9\%$  after 14 days (Fig. 3C). The morphology and *in vitro* release characteristics of pPB-MSA-loaded microspheres were published before [15].

### 3.4. *In vivo* antifibrotic effects of pPB-MSA-Y27632-loaded microspheres

The microspheres containing pPB-MSA-Y27632 were injected once subcutaneously in Mdr2 $^{-/-}$  mice aged 8–9 weeks, suffering from advanced biliary liver fibrosis. At 7 days after injection, we were able to

detect levels of  $721 \pm 23$  ng platinum/liver, reflecting the presence of the Lx-linker as part of pPB-MSA-Y27632. We performed a gene array on liver samples of these mice, and observed that the gene expression levels for the extracellular matrix proteins (collagens 1a1, 1a2, 3a1, 4a1, 5a1 and 6a1, elastin and fibronectin 1) were significantly reduced ( $p = 0.001$ ) in the group of mice treated with microspheres containing pPB-MSA-Y27632 as compared to mice that received empty microspheres (Fig. 4A). Moreover, gene expression levels for the profibrogenic cytokines (transforming growth factor beta 1 (TGF $\beta$ -1) and platelet-derived growth factor BB (PDGF-BB)) and matrix metalloproteinases MMP-2 and -14 were markedly reduced ( $p = 0.026$  and  $0.021$ , respectively) following treatment with pPB-MSA-Y27632-loaded microspheres as compared to diseased control animals that received empty microspheres (Fig. 4B and C, respectively), as demonstrated by the reduced z-normalized values and the accessory heat maps (expression of the separate genes is shown in Fig. S2). The treatment did not affect the expression levels of proteoglycans (decorin, biglycan and fibromodulin), proinflammatory cytokines (interleukin 1 $\beta$ , tumor necrosis factor and chemokine ligand 2), proteases (cathepsin K, bone morphogenetic protein 1 and ADAMTS2) or protease inhibitors (TIMP2, plasminogen activator inhibitor 1) (data not shown). The antifibrotic effect on ECM proteins was confirmed at the protein level by immunohistochemical staining for collagen I&III, that clearly demonstrated regression of bridging fibrosis in the liver parenchyma of mice treated with pPB-MSA-Y27632-containing microspheres as compared to the control groups (empty MSP or pPB-MSA MSP) or plain Y27632 (Fig. 5A and B).

Free Y27632 injected subcutaneously once daily did not have any antifibrotic effect in the livers of these mice. Previous studies did show an effect of Y27632 on liver fibrosis [7], albeit to a lesser extent than the targeted equivalent, but in these studies free Y27632 was administered intravenously.

## 4. Discussion

Kinase inhibitors seem promising for future treatment of fibrotic diseases, as they inhibit the proliferation and contractility of the key pathogenic cells in liver fibrogenesis, *i.e.* the myofibroblasts including activated hepatic stellate cells (HSCs) [22]. In particular, the rho kinase inhibitor Y27632 was shown both *in vitro* and *in vivo* to effectively reduce fibrotic parameters [9–11,23]. Despite its antifibrotic potential, this kinase inhibitor induced several serious adverse effects [8,12]. Therefore, in our studies we aimed to deliver Y27632 to the HSCs that control the excessive extracellular matrix (ECM) protein deposition and blood flow in the cirrhotic liver. We delivered this compound to the fibrogenic and contractile cells by targeting the highly and specifically expressed PDGF $\beta$ -receptor [24], after attaching multiple Y27632 moieties to the HSC-selective drug carrier pPB-MSA [14,15]. The receptor selectivity and preferential localization of the human equivalent and several similar constructs based on the same targeting moiety were already demonstrated before both *in vitro* and *in vivo* in various studies [14,25,26]. For effective treatment of chronic diseases such as fibrosis we further developed a patient-friendly formulation that could facilitate the gradual and prolonged release of this pPB-MSA-Y27632, thereby circumventing high plasma concentrations following intravenous injections and avoiding multiple administrations [18]. In the present study, we achieved a sustained release of pPB-MSA-Y27632 from polymeric microspheres *in vitro* and moreover demonstrated its prolonged antifibrotic activity *in vivo*.

In *in vitro* experiments assessing HSCs contractility, we demonstrated that pPB-MSA-Y27632 was equally active as free Y27632. Our results are in line with those of previous *in vitro* studies with Y27632-constructs targeted to the PDGF $\beta$ -receptor or the mannose 6-phosphate/insulin-like growth factor II (M6P/IGFII) receptor [7,27]. These results confirm that our protein construct is pharmacologically active and also show that *in vitro* there is no added value to the targeted

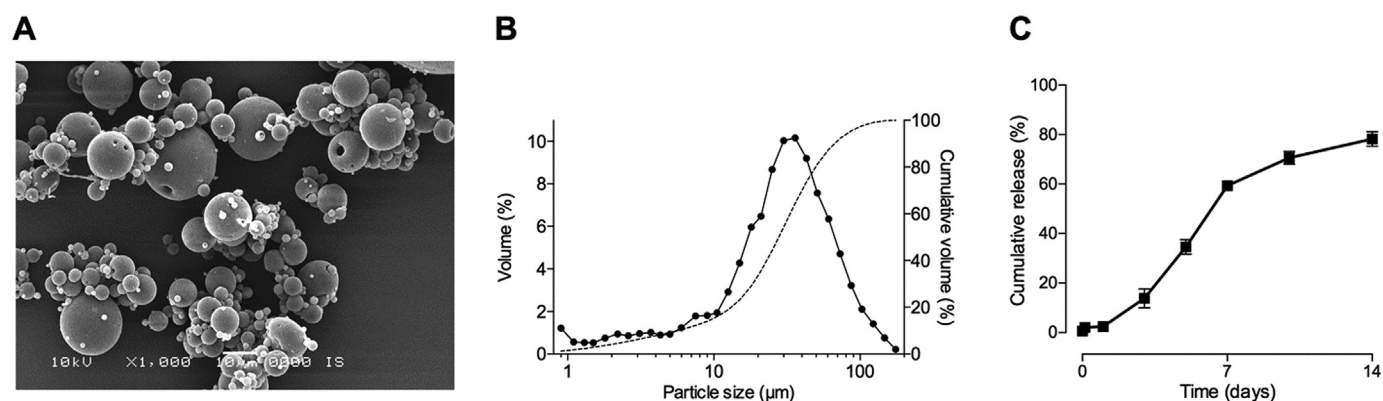


**Fig. 3.** Morphology, particle size distribution and *in vitro* release of proteins from polymeric microspheres containing pPB-MSA-Y27632. (A) Representative scanning electron micrograph of pPB-MSA-Y27632-loaded microspheres after freeze-drying (1000× magnification) showing smooth spherical particles. (B) Particle size distribution of microspheres with volume percentage on left y-axis (solid line) and cumulative volume percentage on right y-axis (dashed line). (C) Cumulative *in vitro* release of proteins from pPB-MSA-Y27632-loaded microspheres as measured with BCA assay. Percentages are corrected for the encapsulation efficiency.

construct as compared to free Y27632.

The used platinum (II)-based Lx-linker, creating a coordinative bond between the rho kinase inhibitor and pPB-MSA, offers advantages in terms of synthesis and stability of the construct [16]. It was previously shown that this linker, when attached to another kinase inhibitor and carrier protein, after endocytosis could provide a local drug reservoir for several days following a single injection assuring slow intracellular release of the drug [16]. This can be explained by the slow ligand-exchange kinetics of platinum allowing replacement of attached drugs by other (intracellular) ligands such as glutathione [28], or by degradation of the protein part of the construct by cellular enzymes in lysosomes, enabling the release of the active compound [16]. Ultimately, all the protein components are degraded. The fate of the Lx-linker is still unknown, but it will most likely form intracellular conjugates with glutathione [29]. Although platinum-based compounds like cisplatin are notorious nephrotoxic agents, this particular platinum (II)-based linker did neither induce any toxicity *in vitro* in amongst others renal tubular cells nor *in vivo* in the kidneys [16]. This is due to the relatively low concentrations of the linker (far below toxicity levels) and to the fact that platinum is not present in its unconjugated (free) form; it is either coupled to albumin or to intracellular ligands like glutathione [29].

Previous studies using the same Lx-linker demonstrated the antifibrotic potential of Y27632 *in vivo* when targeted to the M6P/IGFII-receptor expressed on activated HSCs in the CCl<sub>4</sub> model of parenchymal liver fibrosis [7]. Also, when Y27632 was coupled to the renal-specific protein lysozyme via the aforementioned linker, a significant reduction in renal fibrotic parameters was observed in the ischemia/reperfusion injury rat model [17]. Moreover, a strong inhibition of tubular damage and inflammation was demonstrated.

The rho kinase inhibitor Y27632 was not the only compound that was successfully targeted to fibrotic organs including the liver by coupling to carrier molecules using the platinum-based linker technology. Several studies demonstrated the targeting of other Lx-based constructs to the liver as well, albeit in different species and using animal models of different etiology. The antifibrotic and anti-inflammatory effects of the angiotensin type 1 receptor blocker losartan conjugated to the HSC-

selective drug carrier mannose-6-phosphate modified human serum albumin (M6P-HSA) were demonstrated in rats with advanced liver fibrosis induced by prolonged bile duct ligation or CCl<sub>4</sub> administration [30]. Moreover, the organ specificity of the construct and colocalization with activated HSCs being the target cells were demonstrated. In another study, a tyrosine kinase inhibitor (the imatinib derivative PAP19) was coupled to M6P-HSA using the Lx-linker, in order to reach activated HSCs in the fibrotic liver, where a reduction in collagen deposition and activation of HSCs in livers of bile duct ligated rats was found [31]. Although all described constructs significantly reduced several fibrosis related parameters, the number one choice for the drug to target will ultimately depend on disease etiology.

In the present study we only focused on the antifibrotic effects of our formulation, and did not consider other effects such as inflammation or hemodynamic effects. Our group and others previously demonstrated that the inhibition of rho kinase with Y27632 in activated HSCs using several selective carriers, including M6P-HSA and pPB-HSA, significantly decreased portal pressure and hepatic vascular resistance in different animal models of liver cirrhosis with portal hypertension [4,7,27]. This confirms the importance of rho kinase in the regulation of the hepatic vascular resistance and blood pressure. Selective inhibition of rho kinase did not cause any off-target hemodynamic or toxic effects [4,27]. The effects on portal pressure and fibrosis were explained by a reduction in phosphorylation of myosin light chain (MLC) in HSCs, as one of the downstream proteins in the rho kinase pathway [4,7,27].

For the future treatment of chronic diseases such as liver fibrosis, continuous drug release provided by a sustained release formulation may be crucial in addition to the slow intracellular release governed by the Lx-linker, because high plasma levels possibly leading to toxicity are prevented. Moreover, a discontinuous effect of drugs, in the case for rho kinase inhibitors on for instance portal pressure, may still lead to a perpetuation of disease activity. An additional benefit of a sustained release formulation is that multiple injections are not necessary, and thus patient compliance and comfort are improved [19]. We now were able to show the pharmacological effects of Y27632 one week after a

**Table 2**  
Characteristics of microspheres with different contents used *in vivo* in the Mdr2<sup>−/−</sup> model.

Formulation	Theoretical protein load	Particle size in μm (SEM)			Span	Encapsulation efficiency (%)	Total protein load (%)	Drugload (Y27632, μg)
		X <sub>10</sub>	X <sub>50</sub>	X <sub>90</sub>				
pPB-MSA-Y27632 (PMY)	1% PMY/4% MSA	5.7 (0.1)	27.9 (0.2)	67.1 (0.2)	2.2	80.6	4.1	12.4
pPB-MSA	3% pPB-MSA/2% MSA	3.4 (0.1)	21.6 (0.3)	66.7 (0.7)	2.9	103.3	5.2	–
Control	–	3.1 (0.0)	22.0 (0.2)	63.9 (0.5)	2.8	–	–	–

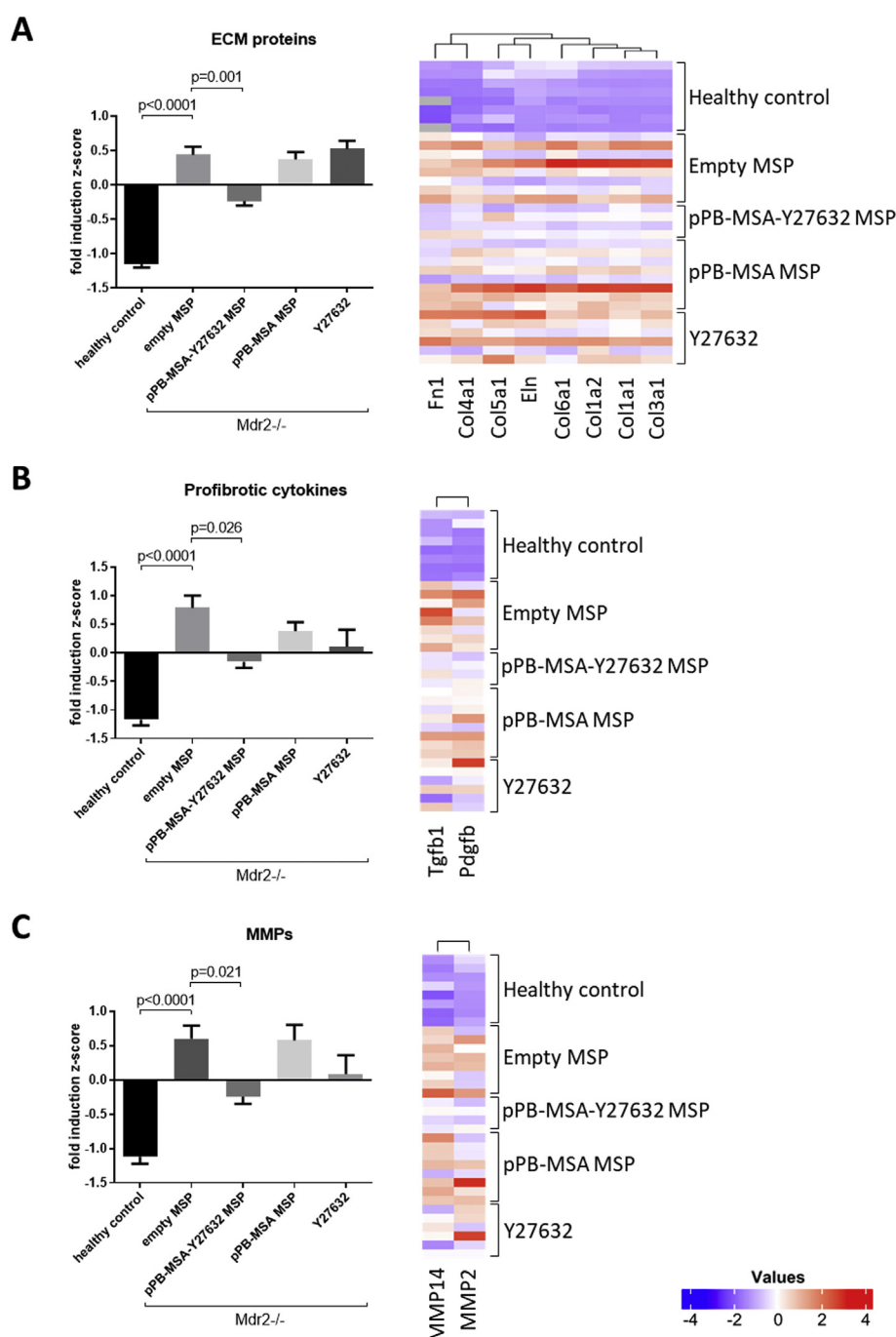


**Fig. 4.** *In vivo* effects of pPB-MSA-Y27632 released from subcutaneously residing polymeric microspheres on the gene level. Z-normalized values of fold inductions (fold inductions are relative to healthy controls) and heat maps of (A) extracellular matrix proteins (collagens 1a1, 1a2, 3a1, 4a1, 5a1 and 6a1, elastin and fibronectin 1), (B) profibrogenic cytokines (TGFβ-1 and PDGF-BB) and (C) matrix metalloproteinases (MMP-2 and -14) at mRNA level in the different treatment groups. Two missing z-normalized values for fibronectin 1 are depicted in grey.

single subcutaneous injection by applying polymeric microspheres containing pPB-MSA-Y27632. Thus, by incorporating a high molecular weight cell-specific protein in microspheres that enable slow release, an effective concentration on the target site can be achieved.

The polymeric microsphere formulation was found suitable for the sustained release of large therapeutic proteins in previous studies. The polymers that were used to produce the microspheres are biodegradable phase-separated multi-block copolymers, composed of poly(L-lactide) (PLLA), poly ethylene glycol (PEG) and poly(ε-caprolactone) (PCL), of which the *in vivo* biocompatibility was shown not to be different from poly(lactic-co-glycolic acid) (PLGA), the FDA-approved

golden standard [33]. Although macrophage infiltration into the implantation site occurred over time as part of the foreign body response, this did not seem to have an effect on the functionality of the microspheres (unpublished data). We studied the *in vivo* release kinetics of a similar carrier protein encapsulated in such microspheres, which most likely reaches the systemic circulation via the lymphatic system, and subsequent localization in the unilateral ureter obstruction (UUO) model for kidney fibrosis and the Mdr2<sup>-/-</sup> model for liver fibrosis before [15,20].

We proceeded with the same formulation and now encapsulated pPB-MSA-Y27632, which showed *in vitro* diffusion-controlled sustained

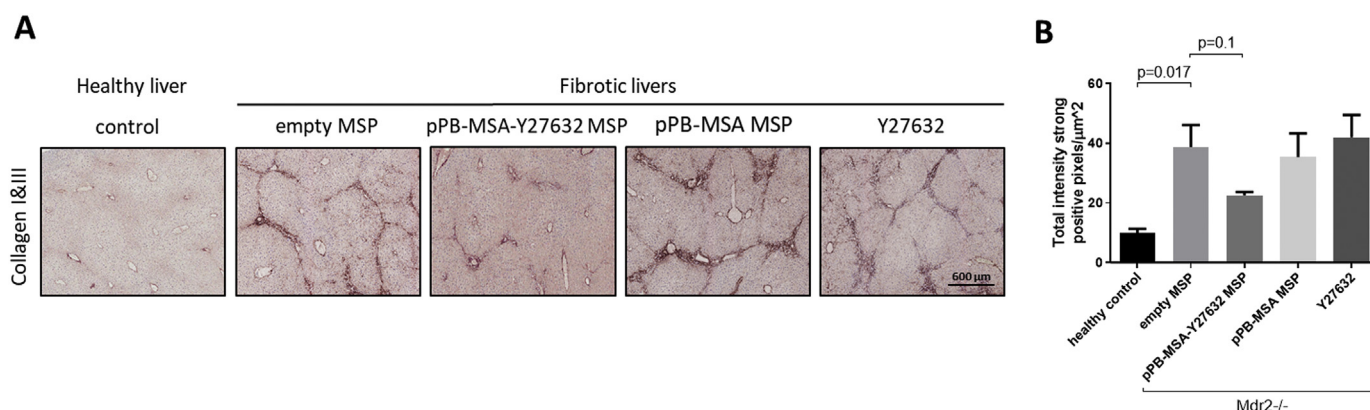


**Fig. 5.** *In vivo* effects of pPB-MSA-Y27632 released from microspheres on the protein expression of collagens I&III. (A) Immunohistochemical staining and (B) quantification for collagens I&III in *Mdr2*<sup>-/-</sup> livers of mice at 7 days after microsphere injection containing pPB-MSA-Y27632 or controls. The distribution was tested for normality with Shapiro-Wilk test, after which differences between groups were assessed by one-way ANOVA followed by Benjamini-Hochberg correction.

release for at least 14 days. The platinum concentration reached in the liver was  $721 \pm 23$  ng/liver, reflecting the amount platinum conjugated to the carrier plus the amount of platinum conjugated to intracellular products (most likely glutathione conjugates) following the release of Y27632 from the carrier. The steady state concentration in the fibrotic livers of mice that received microspheres containing pPB-HSA was  $121 \pm 28.3$  ng/liver, as determined by ELISA in a previous study [15], which is in the same range given the fact that 5 molecules of Y27632 are attached to each carrier molecule. Since our main objective was to demonstrate the presence of our construct in the liver using ICP-MS rather than to prove specific targeting, we did not consider platinum concentrations in off-target organs.

The key question was whether these levels, obtained at the target site after slow release from a subcutaneous depot, were high enough to reach therapeutic concentrations to exert an antifibrotic effect. Clearly, the gene array showed a reduction in gene expression levels of several ECM proteins, profibrotic cytokines and matrix metalloproteinases (MMPs), and additionally a decrease in collagen I&III protein expression in *Mdr2*<sup>-/-</sup> mice that received microspheres containing pPB-MSA-Y27632. These data convincingly demonstrate an important pharmacological effect of Y27632 at the target site.

The mechanism of the antifibrotic effect of Y27632 may be very complex. According to all our gene array data, this could either be related to the reduced expression of profibrotic cytokines, or the consequence of reduced expression of MMPs. Evidently, mechanistic studies at the protein level are necessary in order to gain more insight in the involved profibrotic and pro-resolution factors. MMPs are involved in the maintenance of the ECM and processes of tissue repair. These proteinases not only resolve the excess matrix, but certain MMPs can have profibrotic functions as well [34]. For example, both MMP-2 and MMP-14 were reported to be antifibrotic via degradation of ECM proteins [34,35], while other studies demonstrated contribution to fibrosis via proliferation of stellate cells [36] or by releasing transforming growth factor beta 1 (TGFβ-1) [37].

In conclusion, we demonstrated that Y27632, when coupled to pPB-MSA and incorporated in subcutaneous polymeric microspheres, is pharmacologically active at the target site, *i.e.* within the fibrotic liver. This pharmacological effect was observed 7 days after the microsphere administration. Equimolar dosages of Y27632 were ineffective, showing the relevance of our combined targeting - sustained release approach. Polymeric microspheres may be suitable for the patient-friendly delivery of therapeutic proteins such as pPB-MSA-Y27632.

## Acknowledgements

The authors thank HendrikJan Houthoff (LinXis BV, Amsterdam) for providing Y27632-Lx, Miriam Boersema (Department of

Pharmaceutical Technology and Biopharmacy) for her help with the low density array, and Imco Sibum for his assistance at the scanning electron microscope. This study was performed using a grant of the Netherlands Institute of Regenerative Medicine (NIRM), a grant from NanoNext.NL (program 03.10), the EU ERC Advanced Grant FIBROIMAGING and a grant from the German Research Foundation (DFG), Collaborative Research Center SFB1066, to Detlef Schuppan.

## Appendix A. Supplementary data

Supplementary data to this article can be found online at <https://doi.org/10.1016/j.jconrel.2018.12.039>.

## References

- [1] J. Bosch, J.C. Garcia-Pagan, Complications of cirrhosis. I. Portal hypertension, *J. Hepatol.* 32 (1 Suppl) (2000) 141–156.
- [2] M. Hennenberg, J. Trebicka, T. Sauerbruch, J. Heller, Mechanisms of extrahepatic vasodilation in portal hypertension, *Gut* 57 (9) (2008) 1300–1314.
- [3] W. Ekataksin, K. Kaneda, Liver microvascular architecture: an insight into the pathophysiology of portal hypertension, *Semin. Liver Dis.* 19 (4) (1999) 359–382.
- [4] S. Klein, M.M. Van Beuge, M. Granzow, et al., HSC-specific inhibition of rho-kinase reduces portal pressure in cirrhotic rats without major systemic effects, *J. Hepatol.* 57 (6) (2012) 1220–1227.
- [5] Q. Zhou, M. Hennenberg, J. Trebicka, et al., Intrahepatic upregulation of RhoA and rho-kinase signalling contributes to increased hepatic vascular resistance in rats with secondary biliary cirrhosis, *Gut* 55 (9) (2006) 1296–1305.
- [6] M. Amano, M. Nakayama, K. Kaibuchi, Rho-kinase/ROCK: a key regulator of the cytoskeleton and cell polarity, *Cytoskeleton (Hoboken)* 67 (9) (2010) 545–554.
- [7] M.M. van Beuge, J. Prakash, M. Lacombe, et al., Reduction of fibrogenesis by selective delivery of a rho kinase inhibitor to hepatic stellate cells in mice, *J. Pharmacol. Exp. Ther.* 337 (3) (2011) 628–635.
- [8] M. Hennenberg, E. Biecker, J. Trebicka, et al., Defective RhoA/rho-kinase signaling contributes to vascular hypocontractility and vasodilation in cirrhotic rats, *Gastroenterology* 130 (3) (2006) 838–854.
- [9] S. Tada, H. Iwamoto, M. Nakamura, et al., A selective ROCK inhibitor, Y27632, prevents dimethylnitrosamine-induced hepatic fibrosis in rats, *J. Hepatol.* 34 (4) (2001) 529–536.
- [10] T. Murata, S. Arai, A. Mori, M. Imamura, Therapeutic significance of Y-27632, a rho-kinase inhibitor, on the established liver fibrosis, *J. Surg. Res.* 114 (1) (2003) 64–71.
- [11] T. Murata, S. Arai, T. Nakamura, et al., Inhibitory effect of Y-27632, a ROCK inhibitor, on progression of rat liver fibrosis in association with inactivation of hepatic stellate cells, *J. Hepatol.* 35 (4) (2001) 474–481.
- [12] T. Force, D.S. Krause, R.A. Van Etten, Molecular mechanisms of cardiotoxicity of tyrosine kinase inhibition, *Nat. Rev. Cancer* 7 (5) (2007) 332–344.
- [13] S.L. Friedman, Mechanisms of hepatic fibrogenesis, *Gastroenterology* 134 (6) (2008) 1655–1669.
- [14] L. Beljaars, B. Weert, A. Geerts, D.K. Meijer, K. Poelstra, The preferential homing of a platelet derived growth factor receptor-recognizing macromolecule to fibroblast-like cells in fibrotic tissue, *Biochem. Pharmacol.* 66 (7) (2003) 1307–1317.
- [15] F. van Dijk, N. Teekamp, L. Beljaars, et al., Pharmacokinetics of a sustained release formulation of PDGFβ-receptor directed carrier proteins to target the fibrotic liver, *J. Control. Release* 269 (2017) 258–265.
- [16] J. Prakash, M. Sandovici, V. Saluja, et al., Intracellular delivery of the p38 mitogen-activated protein kinase inhibitor SB202190 [4-(4-fluorophenyl)-2-(4-



- hydroxyphenyl)-5-(4-pyridyl)1H-imidazole] in renal tubular cells: a novel strategy to treat renal fibrosis, *J. Pharmacol. Exp. Ther.* 319 (1) (2006) 8–19.
- [17] J. Prakash, M.H. de Borst, M. Lacombe, et al., Inhibition of renal rho kinase attenuates ischemia/reperfusion-induced injury, *J. Am. Soc. Nephrol.* 19 (11) (2008) 2086–2097.
- [18] V.W. Steinijans, Pharmacokinetic characterization of controlled-release formulations, *Eur. J. Drug Metab. Pharmacokinet.* 15 (2) (1990) 173–181.
- [19] R. Vaishya, V. Khurana, S. Patel, A.K. Mitra, Long-term delivery of protein therapeutics, *Expert Opin. Drug Deliv.* 12 (3) (2015) 415–440.
- [20] N. Teekamp, F. Van Dijk, A. Broesder, et al., Polymeric microspheres for the sustained release of a protein-based drug carrier targeting the PDGFbeta-receptor in the fibrotic kidney, *Int. J. Pharm.* 534 (1–2) (2017) 229–236.
- [21] C. Cheadle, M.P. Vawter, W.J. Freed, K.G. Becker, Analysis of microarray data using Z score transformation, *J. Mol. Diagn.* 5 (2) (2003) 73–81.
- [22] Y. Koyama, J. Xu, X. Liu, D.A. Brenner, New developments on the treatment of liver fibrosis, *Dig. Dis.* 34 (5) (2016) 589–596.
- [23] K. Nagatoya, T. Moriyama, N. Kawada, et al., Y-27632 prevents tubulointerstitial fibrosis in mouse kidneys with unilateral ureteral obstruction, *Kidney Int.* 61 (5) (2002) 1684–1695.
- [24] E. Borkham-Kamphorst, E. Kovalenko, C.R. van Roeyen, et al., Platelet-derived growth factor isoform expression in carbon tetrachloride-induced chronic liver injury, *Lab. Invest.* 88 (10) (2008) 1090–1100.
- [25] J. Prakash, E. de Jong, E. Post, A.S. Gouw, L. Beljaars, K. Poelstra, A novel approach to deliver anticancer drugs to key cell types in tumors using a PDGF receptor-binding cyclic peptide containing carrier, *J. Control. Release* 145 (2) (2010) 91–101.
- [26] W.I. Hagens, A. Mattos, R. Greupink, et al., Targeting 15d-prostaglandin J2 to hepatic stellate cells: two options evaluated, *Pharm. Res.* 24 (3) (2007) 566–574.
- [27] F. Magdaleno, S. Klein, F. Frohn, C. Reker-Smit, F.E. Uschner, R. Schierwagen, K. Poelstra, L. Beljaars, J. Trebicka, Rho-kinase inhibitor coupled with peptide-modified albumin carrier reduces fibrogenesis and portal pressure in cirrhotic rats without systemic effects, *Hepatology* 66 (142A) (2017).
- [28] K. Ikeda, K. Miura, S. Himeno, N. Imura, A. Naganuma, Glutathione content is correlated with the sensitivity of lines of PC12 cells to cisplatin without a corresponding change in the accumulation of platinum, *Mol. Cell. Biochem.* 219 (1–2) (2001) 51–56.
- [29] T. Gonzalo, E.G. Talman, A. van de Ven, et al., Selective targeting of pentoxifylline to hepatic stellate cells using a novel platinum-based linker technology, *J. Control. Release* 111 (1–2) (2006) 193–203.
- [30] M. Moreno, T. Gonzalo, R.J. Kok, et al., Reduction of advanced liver fibrosis by short-term targeted delivery of an angiotensin receptor blocker to hepatic stellate cells in rats, *Hepatology* 51 (3) (2010) 942–952.
- [31] T. Gonzalo, L. Beljaars, M. van de Bovenkamp, et al., Local inhibition of liver fibrosis by specific delivery of a platelet-derived growth factor kinase inhibitor to hepatic stellate cells, *J. Pharmacol. Exp. Ther.* 321 (3) (2007) 856–865.
- [32] J. Zandstra, Microspheres for Local Drug Delivery (Doctoral Thesis), (2016).
- [33] M. Giannandrea, W.C. Parks, Diverse functions of matrix metalloproteinases during fibrosis, *Dis. Model. Mech.* 7 (2) (2014) 193–203.
- [34] F.G. Spinale, J.S. Janicki, M.R. Zile, Membrane-associated matrix proteolysis and heart failure, *Circ. Res.* 112 (1) (2013) 195–208.
- [35] R.C. Benyon, C.J. Hovell, M. Da Gaca, E.H. Jones, J.P. Iredale, M.J. Arthur, Progelatinase A is produced and activated by rat hepatic stellate cells and promotes their proliferation, *Hepatology* 30 (4) (1999) 977–986.
- [36] D. Mu, S. Cambier, L. Fjellbirkeland, et al., The integrin alpha(v)beta8 mediates epithelial homeostasis through MT1-MMP-dependent activation of TGF-beta1, *J. Cell Biol.* 157 (3) (2002) 493–507.